

# AN A POSTERIORI ERROR ESTIMATE OF THE OUTER NORMAL DERIVATIVE USING DUAL WEIGHTS\*

SILVIA BERTOLUZZA<sup>†</sup>, ERIK BURMAN<sup>‡</sup>, AND CUIYU HE<sup>§</sup>

**Abstract.** We derive a residual based a-posteriori error estimate for the outer normal derivative of approximations to Poisson’s problem. By analyzing the solution of the adjoint problem, we show that error indicators in the bulk may be defined to be of higher order than those close to the boundary, which lead to more economic meshes. The theory is illustrated with some numerical examples.

**Key words.** a posteriori error estimate; normal flux; dual weighted residual method

**AMS subject classifications.** 65M50, 65M60

Let  $\Omega \subset \mathbb{R}^2$  be a polygonal domain, let  $\Gamma = \partial\Omega$  denote its boundary and  $\nu$  the outer unit normal. We consider Poisson’s equation

$$-\Delta u = f, \text{ in } \Omega,$$

with Dirichlet boundary conditions,  $u = g$  on  $\Gamma$ . The outer normal derivative  $\nu \cdot \nabla u$  is an important quantity in many applications. It is of importance for instance when a heat flux or an electric field on the boundary of the domain needs to be approximated, or in fluid mechanics for the fluid forces [1, 20, 23, 15]. For boundary control problems, an accurate approximation of the normal derivative on the boundary also plays a critical role [2, 3]. Recently there has been a number of works estimating the error for the outer normal derivative in the a priori sense. We refer to [21, 22].

From the computational perspective it is appealing to apply adaptive methods that concentrate degrees of freedom where they are most needed to achieve a certain accuracy. In particular, for the normal derivative on the boundary, we expect perturbations in the bulk of the domain to be less significant than those close to the boundary. This is proved in [10] where local a priori error estimates were given for the error in the outer normal derivative. In particular, the error on the flux quantity was shown to depend on the  $H^1$ -error in a tubular neighborhood of the boundary and a global term that measures the global error in a weak norm. Similar results using boundary concentrated meshes were obtained more recently in [25], where the application to a Dirichlet boundary control problem was studied. A consequence of the localization property underlying the above a priori error estimates is that a standard energy norm estimate is unlikely to have optimal performance when approximating the normal flux, since it does not account for the relative independence of the goal quantity on perturbations in the bulk.

The objective of the present work is to derive a residual based a posteriori error estimate for the outer normal derivative that exploits the localization property. In particular, we add some mesh dependent weight in front of the classical residual based error estimator, and the weights greatly depend on the distance to the boundary. More precisely, the domain is divided into two zones, a tubular neighborhood around the boundary and an interior, bulk zone. For elements in the latter, the residual estimator is multiplied with the mesh diameter to a higher power than in the

---

\*

**Funding:** EB and CH were funded by the EPSRC grant EP/P01576X/1.

<sup>†</sup>Istituto di Matematica Applicata e Tecnologie Informatiche, CNR, Italy, ([silvia.bertoluzza@imati.cnr.it](mailto:silvia.bertoluzza@imati.cnr.it)).

<sup>‡</sup>Department of Mathematics, University College London, UK, ([e.burman@ucl.ac.uk](mailto:e.burman@ucl.ac.uk)).

<sup>§</sup>Department of Mathematics, University of Georgia, USA, ([cuiyu.he@uga.edu](mailto:cuiyu.he@uga.edu))

boundary region, hence giving it relative smaller weight. To get a precise quantification of the size of the weight we consider an adjoint problem, and characterize its solution using the fundamental solution of Laplace equations. By analyzing the Laplace equations we can determine the rate of decrease of the adjoint solution and its derivatives with increasing distance to the boundary. This then helps provide bounds on the dual weights in the a posteriori error estimate that allows us to decompose the domain in a bulk and boundary subdomain with associated error indicators. The use of adjoint equations for the approximation of fluxes and fluid forces in the dual adjoint method was a popular approach in the Dual Weighted Residual a posteriori error estimation approach (see for instance [6, 7, 19, 5, 8, 26]). In these approaches, however, the dual solution was approximated and, to our knowledge, there is no proof of a goal oriented/dual weighted residual a posteriori error estimate where the local dual weights are rigorously bounded and proven to result in a more efficient estimator than the standard energy estimate. With this work we show that a detailed analysis of the adjoint equation can lead to sharper a posteriori bounds.

An outline of the paper is as follows. First we introduce the weak formulation of our model problem and the associated finite element method in section [section 1](#). In section [section 2](#) we derive the a posteriori error estimate. Then we show in section [section 3](#) how to apply the result to some known stabilized methods, such as the Barbosa-Hughes methods and Nitsche's method. Finally we illustrate the theory with some numerical examples in section [section 4](#).

**1. The Lagrange multiplier formulation of the Dirichlet Problem.** For  $g \in H^{1/2}(\Gamma)$  and  $f \in L^2(\Omega)$  given, we consider the problem of finding  $u \in H^1(\Omega)$ ,  $\lambda \in H^{-1/2}(\Gamma)$  such that for all  $v \in H^1(\Omega)$ ,  $\mu \in H^{-1/2}(\Gamma)$

$$(1.1) \quad \int_{\Omega} \nabla u \cdot \nabla v - \int_{\Gamma} \lambda v = \int_{\Omega} f v, \quad \int_{\Gamma} u \mu = \int_{\Gamma} g \mu.$$

We consider a Galerkin discretization of such problem. More precisely, letting  $V_h \subset H^1(\Omega)$ ,  $\Lambda_h \subset H^{-1/2}(\Gamma)$  be finite element spaces defined on a shape regular (but not necessarily quasi uniform) triangulation  $\mathcal{T}_h$ , we look for  $u_h \in V_h$ ,  $\lambda_h \in \Lambda_h$  such that for all  $v_h \in V_h$ ,  $\mu_h \in \Lambda_h$

$$(1.2) \quad \int_{\Omega} \nabla u_h \cdot \nabla v_h - \int_{\Gamma} \lambda_h v_h = \int_{\Omega} f v_h, \quad \int_{\Gamma} u_h \mu_h = \int_{\Gamma} g \mu_h.$$

We assume that  $V_h$  contains the space of continuous piecewise polynomials of order  $k$  on  $\mathcal{T}_h$ , which we denote by  $\tilde{V}_h$ , and that  $\Lambda_h$  contains a subspace  $\tilde{\Lambda}_h$  which is either the space of piecewise constants, or the space of continuous piecewise linears on the mesh induced on  $\Gamma$  by  $\mathcal{T}_h$ .

Restricting the test functions in (1.1) to the discrete spaces and taking the difference of (1.1) and (1.2) we see that the following Galerkin orthogonality holds: for all  $v_h \in V_h$ ,  $\mu_h \in \Lambda_h$

$$(1.3) \quad \int_{\Omega} \nabla(u - u_h) \cdot \nabla v_h - \int_{\Gamma} (\lambda - \lambda_h) v_h = 0, \quad \int_{\Gamma} (u - u_h) \mu_h = 0.$$

*Remark 1.1.* Observe that in the above we are as general as possible in the definition of the two spaces. We do not even need to assume that the spaces satisfy the inf-sup condition. This of course does not mean that the method is stable without it, only that the a posteriori error estimate will measure the computational error independently of the stability properties of the pair  $V_h \times \Lambda_h$ . An example of spaces that may be used in the framework are

$$V_h = \{u \in H^1(\Omega) : u|_T \in \mathbb{P}_k(T), \forall T \in \mathcal{T}_h\},$$

and, for  $k' \geq 0$

$$\Lambda_h = \{\lambda \in L^2(\Gamma) : u|_e \in \mathbb{P}_{k'}(e), \forall e \in \mathcal{T}_h|_\Gamma\},$$

or, for  $k' \geq 1$

$$\Lambda_h = \{\lambda \in C^0(\Gamma) : u|_e \in \mathbb{P}_{k'}(e), \forall e \in \mathcal{T}_h|_\Gamma\}.$$

Also variants of these spaces with local conforming enrichment on the boundary to satisfy the inf-sup condition are valid [12]. Remark that, when, as in our case, the domain has corners, this last space will not have optimal approximation for the multiplier, and it should be modified following the strategy used in the mortar method (see [9]), where discontinuity is allowed at the corners, with  $k' = k$  in the elements interior to the edges, while in the elements adjacent to the corners  $k' = k - 1$ . Observe, however, that also for the suboptimal choice, the estimator we are going to present, remains valid.

**2. A posteriori error estimates.** The a posteriori error estimate is derived in three steps. We first derive an error representation using the adjoint problem. We then derive the local bounds for the adjoint solution and, finally, we obtain the weighted residual estimates. In what follows we will use the notation  $A \lesssim B$  to indicate that  $A \leq cB$  for some positive constant  $c$  independent of mesh size parameters such as element diameters and edge lengths.  $A \simeq B$  will stand for  $A \lesssim B \lesssim A$ .

**2.1. Error representation using duality.** We let

$$A : (H^1(\Omega) \times H^{-1/2}(\Gamma)) \times (H^1(\Omega) \times H^{-1/2}(\Gamma)) \rightarrow \mathbb{R}$$

be defined by

$$(2.1) \quad A(w, \eta; v, \zeta) = \int_{\Omega} \nabla w \cdot \nabla v - \int_{\Gamma} \eta v + \int_{\Gamma} w \zeta.$$

Let  $(u, \lambda) \in H^1(\Omega) \times H^{-1/2}(\Gamma)$  be the solution of (1.1) and let  $(u_h, \lambda_h) \in V_h \times \Lambda_h$  satisfy (1.2). Set  $e = u - u_h$ ,  $\delta = \lambda - \lambda_h$ . We define  $L : H^{-1/2}(\Gamma) \rightarrow \mathbb{R}$  as

$$L(\xi) := \|\delta\|_{-1/2, \Gamma}^{-1}(\delta, \xi)_{-1/2, \Gamma}, \quad \text{so that} \quad L(\delta) = \|\delta\|_{-1/2, \Gamma},$$

where  $(\cdot, \cdot)_{-1/2, \Gamma}$  is the scalar product for the space  $H^{-1/2}(\Gamma)$ , whose precise expression we will provide later in (2.5), and where  $\|\cdot\|_{-1/2, \Gamma}$  is the corresponding norm. Define  $(z, \zeta) \in \mathcal{V} = H^1(\Omega) \times H^{-1/2}(\Gamma)$  as the solution to

$$(2.2) \quad A(w, \eta; z, \zeta) = L(\eta), \quad \forall (w, \eta) \in \mathcal{V}.$$

It is easy to see that  $|L(\xi)| \leq \|\xi\|_{-1/2, \Gamma}$ , then the operator  $L$  has unitary norm. Therefore, by the stability of (2.2), we have

$$(2.3) \quad \|z\|_{1, \Omega} \lesssim 1, \quad \|\zeta\|_{-1/2, \Gamma} \lesssim 1.$$

Let  $\mathcal{E}_h^i$  and  $\mathcal{E}_h^b$  respectively denote the set of interior and boundary edges of the triangulation  $\mathcal{T}_h$  and, for a triangle  $T \in \mathcal{T}_h$ , let  $\nu_T$  denote the outer unit normal to  $\partial T$ . On an edge  $e = \partial T^+ \cap \partial T^-$  we define the jump of the normal derivative by  $[[\nabla u_h \cdot \nu]] = \nabla u_h^+ \cdot \nu_{T^+} + \nabla u_h^- \cdot \nu_{T^-}$ .

PROPOSITION 2.1. (*Error representation*) Let  $\delta = \lambda - \lambda_h$  and let  $z, \zeta$  be the solution of (2.2). Then it holds that for any  $z_h \in V_h$  and  $\zeta_h \in \Lambda_h$

$$(2.4) \quad \begin{aligned} \|\delta\|_{-1/2,\Gamma} &= \sum_{T \in \mathcal{T}_h} \int_T (f + \Delta u_h)(z - z_h) - \sum_{e \in \mathcal{E}_h^i} \int_e \llbracket \nabla u_h \cdot \nu \rrbracket (z - z_h) \\ &+ \sum_{e \in \mathcal{E}_h^b} \int_e (\lambda_h - \partial_\nu u_h)(z - z_h) + \int_\Gamma (g - u_h)(\zeta - \zeta_h). \end{aligned}$$

*Proof.* Taking  $w = e$  and  $\eta = \delta$  in (2.2) we have

$$\|\delta\|_{-1/2,\Gamma} = L(\delta) = A(e, \delta; z, \zeta).$$

Now, for  $z_h \in V_h$ ,  $\zeta_h \in \Lambda_h$  arbitrary, thanks to Galerkin orthogonality (1.3) we can write:

$$\|\delta\|_{-1/2,\Gamma} = A(e, \delta; z - z_h, \zeta - \zeta_h) = I + II$$

with

$$I = \int_\Omega \nabla e \cdot \nabla (z - z_h), \quad II = - \int_\Gamma (\partial_\nu u - \lambda_h)(z - z_h) + \int_\Gamma (g - u_h)(\zeta - \zeta_h).$$

For the term  $I$  we obtain using Green's theorem

$$\begin{aligned} I &= \int_\Omega \nabla e \cdot \nabla (z - z_h) = \sum_{T \in \mathcal{T}_h} \int_T \nabla e \cdot \nabla (z - z_h) \\ &= \sum_{T \in \mathcal{T}_h} \left( \int_T (f + \Delta u_h)(z - z_h) + \int_{\partial T} \nabla (u - u_h) \cdot \nu_T (z - z_h) \right) \\ &= \sum_T \int_T (f + \Delta u_h)(z - z_h) - \sum_{e \in \mathcal{E}_h^i} \int_e \llbracket \nabla u_h \cdot \nu \rrbracket (z - z_h) \\ &+ \sum_{e \in \mathcal{E}_h^b} \int_e (\partial_\nu u - \partial_\nu u_h)(z - z_h). \end{aligned}$$

Combining all yields (2.4). This completes the proof of the proposition.  $\square$

**2.1.1. Some observations on the operator  $L$ .** We start by observing that taking  $v_h = 1$  in (1.3) there holds  $\int_\Gamma \delta = 0$ . Then we have

$$\|\delta\|_{-1/2,\Gamma} = \sup_{\phi \in H^{1/2}(\Gamma)} \frac{\int_\Gamma \delta \phi}{\|\phi\|_{1/2,\Gamma}} \simeq \sup_{\substack{\phi \in H^{1/2}(\Gamma) \\ \int_\Gamma \phi = 0}} \frac{\int_\Gamma \delta \phi}{|\phi|_{1/2,\Gamma}}.$$

On the space  $H_0^{1/2}(\Gamma) = \{\phi \in H^{1/2} : \int_\Gamma \phi = 0\}$  of zero average functions in  $H^{1/2}(\Gamma)$ , we can define a scalar product and a norm, equivalent to the standard  $H^{1/2}$  scalar product and norm, as

$$(\phi, \psi)_{1/2,\Gamma} = \int_\Omega \nabla \phi^{\mathcal{H}} \cdot \nabla \psi^{\mathcal{H}}, \quad |\phi|_{1/2,\Gamma} := |\phi^{\mathcal{H}}|_{1,\Omega},$$

where  $\phi^{\mathcal{H}} \in H^1(\Omega)$  denotes the harmonic lifting of  $\phi$ . We then let  $\|\cdot\|_{-1/2,\Gamma}$  be defined by duality with respect to the above norm. We now let  $\mathfrak{R} : (H^1_{\circ}(\Gamma))' \rightarrow H^1_{\circ}(\Gamma)$  denote the Riesz isomorphism, which, we recall, is defined as the solution to

$$(\mathfrak{R}\lambda, \phi)_{1/2,\Gamma} = \int_{\Gamma} \lambda \phi \quad \forall \phi \in H^1_{\circ}(\Gamma).$$

We recall that, as  $\mathfrak{R}$  is an isomorphism, we also have that

$$(2.5) \quad (\lambda, \mu)_{-1/2,\Gamma} = (\mathfrak{R}\lambda, \mathfrak{R}\mu)_{1/2,\Gamma} = \int_{\Omega} \nabla(\mathfrak{R}\lambda)^{\mathcal{H}} \cdot \nabla(\mathfrak{R}\mu)^{\mathcal{H}}.$$

It is now easy to check that, if  $\mu \in L^2(\Gamma)$  satisfies  $\int_{\Gamma} \mu = 0$ , then  $(\mathfrak{R}\mu)^{\mathcal{H}}$  is the unique solution to

$$(2.6) \quad -\Delta(\mathfrak{R}\mu)^{\mathcal{H}} = 0 \text{ in } \Omega, \quad \int_{\Gamma} (\mathfrak{R}\mu)^{\mathcal{H}} = 0, \quad \partial(\mathfrak{R}\mu)^{\mathcal{H}}/\partial\nu = \mu.$$

Indeed for any function  $v \in H^1(\Omega)$ , there is a unique decomposition  $v = \bar{v} + v_1 + v_0$  such that  $\bar{v} = |\Gamma|^{-1} \int_{\Gamma} v$ ,  $v_0 \in H^1_{\circ}(\Gamma)$  is the harmonic extension of  $v - \bar{v}$ , and  $v_1 \in H^1_0(\Omega)$  satisfies  $\Delta v_1 = \Delta v$ . Then we have that for any  $v \in H^1(\Omega)$

$$(2.7) \quad \int_{\Omega} \nabla(\mathfrak{R}\mu)^{\mathcal{H}} \cdot \nabla v = \int_{\Omega} \nabla(\mathfrak{R}\mu)^{\mathcal{H}} \cdot \nabla v_0 = (\mathfrak{R}\mu, v_0)_{1/2} = \int_{\Gamma} \mu v_0 = \int_{\Gamma} \mu v,$$

which is the weak form of equation (2.6).

**2.2. Local estimates for the adjoint solution  $z$ .** We observe that  $z$  is the solution of the following problem.

$$\int_{\Omega} \nabla w \cdot \nabla z + \int_{\Gamma} w \zeta = 0, \quad - \int_{\Gamma} \eta z = \|\delta\|_{-1/2,\Gamma}^{-1} (\delta, \eta)_{-1/2,\Gamma} = |\mathfrak{R}\delta|_{1/2,\Gamma}^{-1} \int_{\Gamma} \eta \mathfrak{R}\delta.$$

This rewrites as

$$-\Delta z = 0 \text{ in } \Omega, \quad z = -|\mathfrak{R}\delta|_{1/2,\Gamma}^{-1} \mathfrak{R}\delta \text{ on } \Gamma,$$

As a consequence the solution of the adjoint equation is the harmonic extension of a boundary data depending on the boundary error  $\delta$ , i.e.,

$$z = -|\mathfrak{R}\delta|_{1/2,\Gamma}^{-1} (\mathfrak{R}\delta)^{\mathcal{H}}$$

and, by (2.6), it holds that

$$\frac{\partial z}{\partial \nu} = -\|\delta\|_{-1/2,\Gamma}^{-1} \delta \quad \text{on } \Gamma.$$

Now let  $x \in \Omega$ , and let  $\Phi$  denote the fundamental solution of the Laplace equation:

$$(2.8) \quad \Phi(x) = -\frac{1}{2\pi} \log(|x|).$$

The function  $z$  and its derivatives can be expressed using the fundamental solution as follows [16],

$$(2.9) \quad z(x) = \int_{\Gamma} \left( \Phi(y-x) \frac{\delta(y)}{\|\delta\|_{-1/2,\Gamma}} - \nabla \Phi(y-x) \cdot \nu(y) \frac{\mathfrak{R}\delta}{|\mathfrak{R}\delta|_{1/2,\Gamma}} \right) dy,$$

$$(2.10) \quad \frac{\partial^{|\alpha|}}{\partial x^{\alpha}} z(x) = \int_{\Gamma} \left( \frac{\partial^{|\alpha|}}{\partial x^{\alpha}} \Phi(y-x) \frac{\delta(y)}{\|\delta\|_{-1/2,\Gamma}} - \nabla \left( \frac{\partial^{|\alpha|}}{\partial x^{\alpha}} \Phi(y-x) \right) \cdot \nu(y) \frac{\mathfrak{R}\delta}{|\mathfrak{R}\delta|_{1/2,\Gamma}} \right) dy.$$

The idea is now to derive local bounds on  $z$  and its derivatives, by first deriving bounds on the fundamental solution (2.8) and then exploiting them in the identities (2.9) and (2.10). The key results is the following bound for the fundamental solution.

PROPOSITION 2.2. *Let  $B_r$  denote the ball of center  $x = 0$  and radius  $r$ . Then, for any integer  $m \geq 1$  it holds*

$$|\Phi|_{m, \mathbb{R}^2 \setminus B_r} \lesssim r^{1-m}.$$

*Proof.* We start by proving that for  $m \geq 1$  all the derivatives of order  $m$  of  $\Phi$  take the form

$$(2.11) \quad \frac{\partial^{|\alpha|}}{\partial x^\alpha} \Phi(x) = \frac{q_\alpha(x)}{|x|^{2m}}, \quad q_\alpha(x_1, x_2) = \sum_{i=0}^m c_i^\alpha x_1^i x_2^{m-i},$$

i.e.,  $q_\alpha$  is an homogeneous polynomial of order  $m$ . We prove the result by induction on  $m$ . For  $m = 1$ , by direct computation we have that

$$\frac{\partial}{\partial x_1} \Phi(x) = -\frac{1}{2\pi} \frac{x_1}{|x|^2}, \quad \frac{\partial}{\partial x_2} \Phi(x) = -\frac{1}{2\pi} \frac{x_2}{|x|^2}.$$

Let us then assume that for all  $\alpha$  with  $|\alpha| = m$  the  $\alpha$  derivative of  $\Phi$  takes the form (2.11). Now, by direct computation we have

$$\frac{\partial}{\partial x_1} \left( \frac{x_1^i x_2^{m-i}}{(x_1^2 + x_2^2)^m} \right) = \frac{i x_1^{i+1} x_2^{m-i} + i x_1^{i-1} x_2^{m+2-i} - 2m x_1^{i+1} x_2^{m-i}}{(x_1^2 + x_2^2)^{m+1}}.$$

Switching the role of  $x_1$  and  $x_2$ , we obtain an analogous identity for the partial derivative  $\partial/\partial x_2$ . We therefore have (2.11) for  $|\alpha| = m + 1$ .

As we have that  $|x_1^i x_2^{m-i}| \leq |x|^m$  we immediately get the bound

$$\left| \frac{\partial^{|\alpha|}}{\partial x^\alpha} \Phi(x) \right| \lesssim \frac{1}{|x|^m}.$$

We further have the bound

$$|\Phi|_{m, \mathbb{R}^2 \setminus B_r}^2 = \sum_{|\alpha|=m} \int_{\mathbb{R}^2 \setminus B_r} \left| \frac{\partial^{|\alpha|}}{\partial x^\alpha} \Phi(x) \right|^2 \lesssim \int_{\mathbb{R}^2 \setminus B_r} \frac{1}{|x|^{2m}} \lesssim r^{2-2m},$$

where the last bound can be obtained by a direct computation.  $\square$

The above proposition entails the desired bounds for  $z$  and its derivatives, as stated by the following corollary.

COROLLARY 2.3. *Let  $d_\Gamma(x)$  denote the distance of  $x$  from  $\Gamma$ , and let  $z$  be the solution of (2.2). It holds that for any  $T \subset \Omega$*

$$(2.12) \quad |z|_{m, \infty, T} \lesssim \left( \min_{x \in T} d_\Gamma(x) \right)^{-m-1}, \quad |z|_{m, T} \lesssim |T|^{1/2} \left( \min_{x \in T} d_\Gamma(x) \right)^{-m-1}.$$

*Proof.* Let  $x \in K$ . Consider a weight  $\omega_x \in W^{2,\infty}(\Omega)$  with the following characteristics: letting  $B_0 = B(x, d_\Gamma(x)/3)$  (resp.  $B_1 = B(x, 2d_\Gamma(x)/3)$ ) denote the ball of center  $x$  and radius  $d_\Gamma(x)/3$  (resp.  $2d_\Gamma(x)/3$ ),  $\omega_x$  satisfies

$$(2.13) \quad \begin{aligned} \omega_x &= 0, \quad \text{in } B_0, & \omega_x &= 1, \quad \text{in } \Omega \setminus B_1, & 0 \leq \omega_x \leq 1, & \text{in } \Omega, \\ \|\omega_x\|_{1,\infty} &\lesssim d_\Gamma(x)^{-1}, & \|\omega_x\|_{2,\infty} &\lesssim d_\Gamma(x)^{-2}. \end{aligned}$$

Letting  $\Phi_x(y) = \Phi(y - x)$ . From (2.9), (2.10), using a standard duality bound we have

$$(2.14) \quad \left| \frac{\partial^{|\alpha|}}{\partial x^\alpha} z(x) \right| \lesssim \left| \frac{\partial^{|\alpha|}}{\partial x^\alpha} \Phi_x \right|_{1/2,\Gamma} + \left\| \nabla \left( \frac{\partial^{|\alpha|}}{\partial x^\alpha} \Phi_x \right) \cdot \nu \right\|_{-1/2,\Gamma}.$$

To bound the first term in (2.14), using the properties for  $\omega_x$  give that for  $|\alpha| = m$

$$(2.15) \quad \begin{aligned} \left| \frac{\partial^{|\alpha|}}{\partial x^\alpha} \Phi_x \right|_{1/2,\Gamma} &\lesssim \left\| \nabla \left( \omega_x \frac{\partial^{|\alpha|}}{\partial x^\alpha} \Phi_x \right) \right\|_{0,\Omega} \leq \left\| \omega_x \nabla \left( \frac{\partial^{|\alpha|}}{\partial x^\alpha} \Phi_x \right) \right\|_{0,\Omega} + \left\| \nabla \omega_x \left( \frac{\partial^{|\alpha|}}{\partial x^\alpha} \Phi_x \right) \right\|_{0,\Omega} \\ &\lesssim \left\| \nabla \left( \frac{\partial^{|\alpha|}}{\partial x^\alpha} \Phi_x \right) \right\|_{0,\Omega \setminus B_0} + \|\omega_x\|_{1,\infty} \left\| \frac{\partial^{|\alpha|}}{\partial x^\alpha} \Phi_x \right\|_{0,\Omega \setminus B_0} \\ &\lesssim d_\Gamma(x)^{-m} + d_\Gamma(x)^{-1} d_\Gamma(x)^{1-m} \lesssim d_\Gamma(x)^{-m}. \end{aligned}$$

For the second term in (2.14), applying the trace inequality

$$(2.16) \quad \left\| \nabla \left( \frac{\partial^{|\alpha|}}{\partial x^\alpha} \Phi_x \right) \cdot \nu \right\|_{-1/2,\Gamma} \lesssim \left\| \nabla \left( \omega_x \frac{\partial^{|\alpha|}}{\partial x^\alpha} \Phi_x \right) \right\|_{0,\Omega} + \left\| \Delta \left( \omega_x \frac{\partial^{|\alpha|}}{\partial x^\alpha} \Phi_x \right) \right\|_{0,\Omega}.$$

The first term on the right hand side of (2.16) can be bounded the same way as in (2.15). To bound the second term we observe that, in  $\Omega \setminus B_0$  we have that

$$\Delta \left( \frac{\partial^{|\alpha|}}{\partial x^\alpha} \Phi_x \right) = \frac{\partial^{|\alpha|}}{\partial x^\alpha} (\Delta \Phi_x) = 0.$$

This implies that

$$(2.17) \quad \Delta \left( \omega_x \frac{\partial^{|\alpha|}}{\partial x^\alpha} \Phi_x \right) = \left( \frac{\partial^{|\alpha|}}{\partial x^\alpha} \Phi_x \right) \Delta \omega_x + \nabla \omega_x \cdot \nabla \left( \frac{\partial^{|\alpha|}}{\partial x^\alpha} \Phi_x \right).$$

Then by (2.16)-(2.17), the Cauchy Schwarz inequality, and (2.13) we have

$$(2.18) \quad \begin{aligned} \left\| \nabla \left( \frac{\partial^{|\alpha|}}{\partial x^\alpha} \Phi_x \right) \cdot \nu \right\|_{-1/2,\Gamma} &\lesssim \left\| \nabla \left( \omega_x \frac{\partial^{|\alpha|}}{\partial x^\alpha} \Phi_x \right) \right\|_{0,\Omega} + \left\| \left( \frac{\partial^{|\alpha|}}{\partial x^\alpha} \Phi_x \right) \Delta \omega_x \right\|_{0,\Omega} + \left\| \nabla \omega_x \cdot \nabla \left( \frac{\partial^{|\alpha|}}{\partial x^\alpha} \Phi_x \right) \right\|_{0,\Omega} \\ &\lesssim d_\Gamma(x)^{-m} + \|\omega_x\|_{2,\infty} \|\Phi_x\|_{m,\Omega \setminus B_0} + \|\omega_x\|_{1,\infty} \|\Phi_x\|_{m+1,\Omega \setminus B_0} \\ &\lesssim d_\Gamma(x)^{-m} + d_\Gamma(x)^{-m-1} \\ &\leq d_\Gamma(x)^{-m-1} \left( 1 + \max_{y \in \Omega} d_\Gamma(y) \right) = d_\Gamma(x)^{-m-1} (1 + C_\Omega), \end{aligned}$$

where  $C_\Omega := \max_{y \in \Omega} d_\Gamma(y)$ . Combing all, we have

$$\left| \frac{\partial^{|\alpha|}}{\partial x^\alpha} z(x) \right| \lesssim d_\Gamma(x)^{-m-1} \quad \forall x \in \Omega,$$

and, hence, (2.12). we obtain the desired bound. □

**2.3. The a posteriori error estimator.** Using the error representation of [Proposition 2.1](#) and the local bounds for the adjoint solution stated in [Corollary 2.3](#), we will now derive the a posteriori error estimation. Comparing to the classical residual based error indicator, our local error indicators for each element/edge are additionally multiplied by local dual weights depend on the distance from the element/edge to the boundary. Let us first introduce some notations that will be useful for the bounds.

We let  $h_T$  (resp.  $h_e$ ) denote the diameter (resp. the length) of an element  $T$  (resp. an edge  $e$ ) in  $\mathcal{T}_h$ . For a given triangle  $T \in \mathcal{T}_h$ ,  $\Delta_T$  denotes the patch of elements that have at least a vertex in common with  $T$ , and  $|\Delta_T|$  its measure. The distance of an element  $T$  to the boundary will be measured using  $\rho_T = \min_{x \in \Delta_T} d_\Gamma(x)$ . That is the shortest distance from the associated patch to the boundary.

From [\(5.3\)](#) in the appendix, there exists a projector  $\hat{\Pi}_h : L^2(\Omega) \rightarrow \check{V}_h$ , such that, for  $1 \leq m \leq k+1$  it holds that

$$(2.19) \quad \|z - \hat{\Pi}_h z\|_{0,T} + h_T |z - \hat{\Pi}_h z|_{1,T} \lesssim h_T^m |z|_{m,\Delta_T}.$$

Using this notation we state some local interpolation bounds for the adjoint solution.

**LEMMA 2.4.** *Let  $z_h = \hat{\Pi}_h z$ , then, for  $m = 1$  and  $m = k+1$ ,  $k \geq 1$ , we have the following two bounds*

$$\|z - z_h\|_{0,T} + h_T |z - z_h|_{1,T} \leq C_1 h_T |z|_{1,\Delta_T}, \quad \|z - z_h\|_{0,T} + h_T |z - z_h|_{1,T} \leq C_2 h_T^{k+1} |\Delta_T|^{1/2} \rho_T^{-(k+2)}.$$

The constants  $C_1$  and  $C_2$  depend on the shape regularity of the mesh.

*Proof.* The left inequality is immediate by [\(2.19\)](#) with  $m = 1$ . The right bound follows by first applying [\(2.19\)](#) with  $m = k+1$  and then using [Corollary 2.3](#) to bound

$$|z|_{k+1,\Delta_T} \lesssim |\Delta_T|^{1/2} \rho_T^{-(k+2)}. \quad \square$$

**THEOREM 2.5.** *Define the following local residuals:*

$$(2.20) \quad \begin{aligned} \mathbf{r}(T) &= h_T \|f + \Delta u_h\|_{0,T}, \quad \forall T \in \mathcal{T}_h, \\ \mathbf{r}_0(e) &= h_e^{1/2} \|[\nabla u_h \cdot \nu]\|_{0,e}, \quad \forall e \in \mathcal{E}_h^i, \\ \mathbf{r}_1(e) &= h_e^{1/2} \|\lambda_h - \partial_\nu u_h\|_{0,e}, \quad \forall e \in \mathcal{E}_h^b, \\ \mathbf{r}_2(e) &= h_e^{1/2} |g - u_h|_{1,e}, \quad \forall e \in \mathcal{E}_h^b. \end{aligned}$$

Then we have

$$(2.21) \quad \|\lambda - \lambda_h\|_{-1/2,\Gamma} \lesssim \sqrt{\sum_{T \in \mathcal{T}_h} \varsigma_T^2 |\mathbf{r}(T)|^2 + \sum_{e \in \mathcal{E}_h^i} \varsigma_e^2 |\mathbf{r}_0(e)|^2 + \sum_{e \in \mathcal{E}_h^b} (|\mathbf{r}_1(e)|^2 + |\mathbf{r}_2(e)|^2)},$$

where the element and edge weights  $\varsigma_T$  and  $\varsigma_e$  are defined by

$$(2.22) \quad \varsigma_T = \min\{C_1, C_2 h_T^k \rho_T^{-(k+2)}\}, \quad \varsigma_e = \min\{\varsigma_T, \varsigma_{T'}\}, \quad \text{with } e = T \cap T'.$$

*Proof.* Let us start by splitting  $\mathcal{T}_h$  as the union of two disjoint sets

$$\mathcal{T}_h^1 = \{T \in \mathcal{T}_h : C_1 \leq C_2 h_T^k \rho_T^{-(k+2)}\}, \quad \mathcal{T}_h^2 = \mathcal{T}_h \setminus \mathcal{T}_h^1.$$



Setting  $z_h = \hat{\Pi}_h z$  and  $\zeta_h = 0$  in the error representation of [Proposition 2.1](#), we have

$$\begin{aligned} \|\delta\|_{-1/2,\Gamma} &= \sum_{T \in \mathcal{T}_h} \int_T (f + \Delta u_h)(z - \hat{\Pi}_h z) - \sum_{e \in \mathcal{E}_h^i} \int_e \llbracket \nabla u_h \cdot \nu \rrbracket (z - \hat{\Pi}_h z) \\ &\quad + \sum_{e \in \mathcal{E}_h^b} \int_e (\lambda_h - \partial_\nu u_h)(z - \hat{\Pi}_h z) + \int_\Gamma (g - u_h) \zeta. \end{aligned}$$

Observe that [Lemma 2.4](#) gives us two error estimates for  $\|z - \hat{\Pi}_h z\|_{0,T}$ , and, depending on whether  $T \in \mathcal{T}_h^1$  or  $T \in \mathcal{T}_h^2$ , we apply the best possible estimate. This yields

$$\begin{aligned} &\sum_{T \in \mathcal{T}_h} \int_T (f + \Delta u_h)(z - \hat{\Pi}_h z) \\ &\lesssim \sum_{T \in \mathcal{T}_h^1} \|f + \Delta u_h\|_{0,T} C_1 h_T |z|_{1,\Delta_T} + \sum_{T \in \mathcal{T}_h^2} \|f + \Delta u_h\|_{0,T} C_2 h_T^{k+1} |\Delta_T|^{1/2} \rho_T^{-(k+2)} \\ &= \sum_{T \in \mathcal{T}_h^1} \varsigma_T \mathbf{r}(T) |z|_{1,\Delta_T} + \sum_{T \in \mathcal{T}_h^2} \varsigma_T \mathbf{r}(T) |\Delta_T|^{1/2} \\ &\leq \sqrt{\sum_{T \in \mathcal{T}_h^1} \varsigma_T^2 |\mathbf{r}(T)|^2} \sqrt{\sum_{T \in \mathcal{T}_h^1} |z|_{1,\Delta_T}^2 + \sum_{T \in \mathcal{T}_h^2} |\Delta_T|}. \end{aligned}$$

Collecting the contributions of  $|\Delta_T|$  and applying [\(2.3\)](#) we have

$$\sum_{T \in \mathcal{T}_h^1} |z|_{1,\Delta_T}^2 + \sum_{T \in \mathcal{T}_h^2} |\Delta_T| \lesssim \|z\|_{1,\Omega}^2 + |\Omega| \lesssim C(\Omega),$$

so that

$$(2.23) \quad \sum_{T \in \mathcal{T}_h} \int_T (f + \Delta u_h)(z - \hat{\Pi}_h z) \lesssim C(\Omega) \sqrt{\sum_{T \in \mathcal{T}_h} \varsigma_T^2 |\mathbf{r}(T)|^2}.$$

A similar argument can be applied for interior edges. Letting  $e \in \mathcal{E}_h^i$ ,  $e \subset \partial T$ , the standard bound holds

$$(2.24) \quad \begin{aligned} \int_e \llbracket \nabla u_h \cdot \nu \rrbracket (z - \hat{\Pi}_h z) &\leq \|\llbracket \nabla u_h \cdot \nu \rrbracket\|_{0,e} \|z - \hat{\Pi}_h z\|_{0,e} \\ &\lesssim \|\llbracket \nabla u_h \cdot \nu \rrbracket\|_{0,e} \left( h_T^{-1/2} \|z - \hat{\Pi}_h z\|_{0,T} + h_T^{1/2} |z - \hat{\Pi}_h z|_{1,T} \right) \leq \|\llbracket \nabla u_h \cdot \nu \rrbracket\|_{0,e} h_T^{1/2} C_1 |z|_{1,\Delta_T}, \end{aligned}$$

as well as the enhanced bound

$$(2.25) \quad \int_e \llbracket \nabla u_h \cdot \nu \rrbracket (z - \hat{\Pi}_h z) \leq \|\llbracket \nabla u_h \cdot \nu \rrbracket\|_{0,e} C_2 h_T^{k+1/2} \rho_T^{-(k+2)} |\Delta_T|^{1/2}.$$

As for the cell contribution to the a posteriori estimate, we can retain, for each edge, the more favorable estimator depending on if the face  $e$  belongs to a triangle in  $\mathcal{T}_h^1$  or  $\mathcal{T}_h^2$ . By similar argument for the element residual term, we have

$$(2.26) \quad - \sum_{e \in \mathcal{E}_h^i} \int_e \llbracket \nabla u_h \cdot \nu \rrbracket (z - \hat{\Pi}_h z) \lesssim C(\Omega) \sqrt{\sum_{e \in \mathcal{E}_h^i} \varsigma_e^2 |\mathbf{r}_0(e)|^2}.$$

The boundary terms are treated in the standard way for any  $e \in \mathcal{E}_h^b$  and  $e \subset \partial T$ ,

$$(2.27) \quad \int_e (\lambda_h - \partial_\nu u_h)(z - \hat{\Pi}_h z) \leq \|\lambda_h - \partial_\nu u_h\|_{0,e} \|z - \hat{\Pi}_h z\|_{0,e} \lesssim \|\lambda_h - \partial_\nu u_h\|_{0,e} h_e^{1/2} |z|_{1,\Delta_T}.$$

Therefore,

$$(2.28) \quad \sum_{e \in \mathcal{E}_h^b} \int_e (\lambda_h - \partial_\nu u_h)(z - \hat{\Pi}_h z) \lesssim \left( \sum_{e \in \mathcal{E}_h^b} h_e \|\lambda_h - \partial_\nu u_h\|_{0,e}^2 \right)^{1/2} \|z\|_{1,\Omega} \leq \left( \sum_{e \in \mathcal{E}_h^b} |\mathbf{r}_1(e)|^2 \right)^{1/2}.$$

By (2.3), the last term can be bounded as

$$\int_\Gamma (g - u_h)\zeta \leq \|g - u_h\|_{1/2,\Gamma} \|\zeta\|_{-1/2,\Gamma} \lesssim \|g - u_h\|_{1/2,\Gamma}.$$

Finally, since  $g - u_h$  is orthogonal to  $\check{\Lambda}_h \subseteq \Lambda_h$ , we can use Lemma 3 of [11] to bound

$$(2.29) \quad \|g - u_h\|_{1/2,\Gamma}^2 \lesssim \sum_{e \in \mathcal{E}_h^b} h_e |g - u_h|_{1,e}^2 = \sum_{e \in \mathcal{E}_h^b} |\mathbf{r}_2(e)|^2.$$

Combing all gives (2.21). This completes the proof of the theorem.  $\square$

### 3. Application to stabilized methods for the imposition of boundary conditions.

In engineering practice it is often advantageous to use a stabilized method instead of choosing the spaces so that the inf-sup condition is satisfied. In this section we show how the proposed framework can be adapted to two of the most well-known stabilised methods, namely the Barbosa-Hughes method [4] and the Nitsche's method [24]. Both the final results and the arguments are in the same spirit as Theorem 2.5 above and therefore we only give sketches of the proofs.

**3.1. Indicators for the Barbosa–Hughes method.** The Barbosa–Hughes discrete problem reads: find  $u_h \in V_h$ ,  $\lambda_h \in \Lambda_h$  such that for all  $v_h \in V_h$ ,  $\mu_h \in \Lambda_h$  it holds that

$$(3.1) \quad \int_\Omega \nabla u_h \cdot \nabla v_h - \int_\Gamma \lambda_h v_h \pm \alpha \sum_{e \in \mathcal{E}_h^b} h_e \int_e (\nabla u_h \cdot \nu - \lambda_h) \nabla v_h \cdot \nu = \int_\Omega f v_h,$$

$$(3.2) \quad \int_\Gamma u_h \mu_h - \alpha \sum_{e \in \mathcal{E}_h^b} h_e \int_e (\nabla u_h \cdot \nu - \lambda_h) \mu_h = \int_\Gamma g \mu_h.$$

Here we use  $\pm$  in front of the stabilization term in (3.1), to indicate that the analysis applies to both the symmetric and antisymmetric version of the method. The functional  $L$  and  $z, \zeta$  are defined as in the previous section. Similarly we have the following error representation by subtracting from (1.1): for arbitrary  $z_h \in V_h$  and  $\zeta_h \in \Lambda_h$  it holds that

$$\begin{aligned} L(\delta) &= \int_\Omega \nabla e \cdot \nabla z - \int_\Gamma \delta z + \int_\Gamma e \zeta \\ &= \int_\Omega \nabla e \cdot \nabla (z - z_h) - \int_\Gamma \delta (z - z_h) + \int_\Gamma e (\zeta - \zeta_h) + \int_\Omega \nabla e \cdot \nabla z_h - \int_\Gamma \delta z_h + \int_\Gamma e \zeta_h \\ &= \int_\Omega \nabla e \cdot \nabla (z - z_h) - \int_\Gamma \delta (z - z_h) + \int_\Gamma e (\zeta - \zeta_h) + \alpha \sum_{e \in \mathcal{E}_h^b} h_e \int_e (\nabla u_h \cdot \nu - \lambda_h) (\zeta_h \mp \nabla z_h \cdot \nu). \end{aligned}$$

From [Proposition 2.1](#), we have

$$(3.3) \quad \begin{aligned} L(\delta) = & \sum_{T \in \mathcal{T}_h} \int_T (f + \Delta u_h)(z - z_h) - \sum_{e \in \mathcal{E}_h^i} \int_e \llbracket \nabla u_h \cdot \nu \rrbracket (z - z_h) + \sum_{e \in \mathcal{E}_h^b} \int_e (\lambda_h - \partial_\nu u_h)(z - z_h) \\ & + \int_\Gamma (g - u_h)(\zeta - \zeta_h) + \alpha \sum_{e \in \mathcal{E}_h^b} h_e \int_e (\nabla u_h \cdot \nu - \lambda_h)(\zeta_h \mp \nabla z_h \cdot \nu). \end{aligned}$$

We again set  $z_h = \hat{\Pi}_h z$ ,  $\zeta_h = 0$ . The first three terms in [\(3.3\)](#) can be bounded using [\(2.23\)](#), [\(2.26\)](#) and [\(2.28\)](#). However, for the fourth term in [\(3.3\)](#), contrary to the previous case, we do not have that  $u_h - g$  is orthogonal to the multiplier space, therefore [\(2.29\)](#) no longer holds. Instead we only have a weaker bound. Letting  $\mathcal{N}_h^b$  denote the set of boundary vertices of the triangulation. And for each  $P \in \mathcal{N}_h^b$  denote by  $\Delta_P \subset \Gamma$  the patch formed by the two boundary edges sharing  $P$  as a vertex, we have that [\[17\]](#)

$$(3.4) \quad \|g - u_h\|_{1/2, \Gamma}^2 \lesssim \sum_{P \in \mathcal{N}_h^b} |u_h - g|_{1/2, \Delta_P}^2 + \sum_{e \in \mathcal{E}_h^b} h_e^{-1} \|u_h - g\|_{0, e}^2.$$

We can further localize the term  $|u_h - g|_{1/2, \Delta_P}^2$ . In order to do so we add and subtract  $g_h^P \in \check{V}_h|_{\Delta_P}$ , where  $g_h^P$  is the  $L^2(\Delta_P)$  projection onto the local space of continuous piecewise linears on the 1-D, two elements mesh  $\mathcal{T}_h|_{\Delta_P}$ , yielding

$$|g - u_h|_{1/2, \Delta_P}^2 \lesssim |u_h - g_h^P|_{1/2, \Delta_P}^2 + |g_h^P - g|_{1/2, \Delta_P}^2,$$

which, combining with the inverse inequality, gives

$$|u_h - g_h^P|_{1/2, \Delta_P}^2 \lesssim h_P^{-1} \|u_h - g_h^P\|_{0, \Delta_P}^2 \simeq \sum_{e \subseteq \Delta_P} h_e^{-1} \|u_h - g_h^P\|_{0, e}^2,$$

Thanks to the fact that  $g - g_h^P$  is orthogonal to the continuous piecewise linear functions, we have

$$|g_h^P - g|_{1/2, \Delta_P}^2 \lesssim \sum_{e \subseteq \Delta_P} h_e |g_h^P - g|_{1, e}^2.$$

We also observe that, for  $P$  a vertex of  $e$

$$\|g - u_h\|_{0, e}^2 \lesssim \|g - g_h^P\|_{0, e}^2 + \|g_h^P - u_h\|_{0, e}^2 \lesssim \sum_{e \subseteq \Delta_P} h_e |g_h^P - g|_{1, e}^2 + \|u_h - g_h^P\|_{0, e}^2.$$

Combining these bounds we easily obtain

$$(3.5) \quad \begin{aligned} \int_\Gamma (g - u_h)\zeta & \leq \|g - u_h\|_{1/2, \Gamma} \|\zeta\|_{-1/2, \Gamma} \lesssim \|g - u_h\|_{1/2, \Gamma} \\ & \lesssim \sqrt{\sum_{P \in \mathcal{N}_h^b} \sum_{e \subseteq \Delta_P} (h_e^{-1} \|u_h - g_h^P\|_{0, e}^2 + h_e |g_h^P - g|_{1, e}^2)} = \sqrt{\sum_{P \in \mathcal{N}_h^b} \sum_{e \subseteq \Delta_P} |\mathbf{r}(e, P)|^2}, \end{aligned}$$

where, for  $P$  a vertex of  $e \in \mathcal{E}_h^b$  we define

$$\mathbf{r}(e, P) = \sqrt{h_e^{-1} \|u_h - g_h^P\|_{0, e}^2 + h_e |g_h^P - g|_{1, e}^2}.$$

Finally, we bound the additional term resulting from the stabilization, namely

$$(3.6) \quad \begin{aligned} \sum_{e \in \mathcal{E}_h^b} h_e \int_e (\nabla u_h \cdot \nu - \lambda_h) (\nabla(\hat{\Pi}_h z) \cdot \nu) &\leq \sqrt{\sum_{e \in \mathcal{E}_h^b} h_e \|\nabla u_h \cdot \nu - \lambda_h\|_{0,e}^2} \sqrt{\sum_{e \in \mathcal{E}_h^b} h_e \|\nabla(\hat{\Pi}_h z) \cdot \nu\|_{0,e}^2} \\ &\lesssim \sqrt{\sum_{e \in \mathcal{E}_h^b} h_e \|\nabla u_h \cdot \nu - \lambda_h\|_{0,e}^2}. \end{aligned}$$

The last bound derives from a standard trace inequality on the element  $T$  associated to the boundary edge  $e$  followed by an inverse inequality and an  $H^1$  stability bound for  $\hat{\Pi}_h$

$$\|\nabla(\hat{\Pi}_h z) \cdot \nu\|_{0,e} \lesssim h_T^{-1/2} \|\nabla(\hat{\Pi}_h z)\|_{0,T} + h_T^{1/2} |\nabla(\hat{\Pi}_h z)|_{1,T} \lesssim h_T^{-1/2} \|\nabla(\hat{\Pi}_h z)\|_{0,T} \lesssim h_T^{-1/2} |z|_{1,\Delta_T},$$

which, together with ((2.3)), yields

$$\sum_{e \in \mathcal{E}_h^b} h_e \|\nabla(\hat{\Pi}_h z) \cdot \nu\|_{0,e}^2 \lesssim \|z\|_{1,\Omega}^2 \lesssim 1.$$

We then have

$$(3.7) \quad \mp \alpha \sum_e h_e \int_e (\nabla u_h \cdot \nu - \lambda_h) (\nabla(\hat{\Pi}_h z) \cdot \nu) \lesssim \alpha \sqrt{\sum_{e \in \mathcal{E}_h^b} |\mathbf{r}_1(e)|^2}$$

where, we recall,  $\mathbf{r}_1(e) = h_e^{1/2} \|\nabla u_h \cdot \nu - \lambda_h\|_{0,e}$ .

Collecting the above bounds we obtain the a posteriori error estimate for the Barbosa–Hughes formulation (3.1)–(3.2):

$$(3.8) \quad \|\lambda - \lambda_h\|_{-1/2,\Gamma}^2 \lesssim \sum_{T \in \mathcal{T}_h} \varsigma_T^2 |\mathbf{r}(T)|^2 + \sum_{e \in \mathcal{E}_h^i} \varsigma_e^2 |\mathbf{r}_0(e)|^2 + (1 + \alpha^2) \sum_{e \in \mathcal{E}_h^b} |\mathbf{r}_1(e)|^2 + \sum_{P \in \mathcal{N}_h^b} \sum_{e \subseteq \Delta_P} |\mathbf{r}(e, P)|^2.$$

**3.2. Indicators for Nitsche’s method.** Let us now consider Nitsche’s method, which reads: find  $u_h \in V_h$  such that for all  $v_h \in V_h$ , there holds

$$(3.9) \quad \begin{aligned} &\int_{\Omega} \nabla u_h \cdot \nabla v_h - \int_{\Gamma} v_h \partial_{\nu} u_h \pm \int_{\Gamma} u_h \partial_{\nu} v_h + \gamma \sum_{e \in \mathcal{E}_h^b} h_e^{-1} \int_e u_h v_h \\ &= \int_{\Omega} f v_h \pm \int_{\Gamma} g \partial_{\nu} v_h + \gamma \sum_{e \in \mathcal{E}_h^b} h_e^{-1} \int_e g v_h. \end{aligned}$$

Following the work of Stenberg [27], Nitsche’s method is equivalent to a Barbosa–Hughes method with the choice  $\Lambda_h = L^2(\Gamma)$ . The solution  $u_h, \lambda_h$  of (3.1)–(3.2) with  $\Lambda_h = L^2(\Gamma)$  verifies that  $u_h$  solves (3.9) with  $\gamma = \alpha^{-1}$ , and we have that, on  $e \subset \Gamma$ ,

$$(3.10) \quad \lambda_h = \partial_{\nu} u_h + \gamma h_e^{-1} (g - u_h).$$

Due to the equivalence,  $L(\delta)$  have the same representation (3.3) with  $\alpha$  replaced by  $\gamma^{-1}$ . With the same choice of  $z_h$  and  $\zeta_h$ , the first and second terms can be bounded using (2.23) and (2.26)

respectively. The fourth term  $\int_{\Gamma}(g - u_h)\zeta$  can be bounded using (3.5). For the remaining terms, observing that

$$\mathbf{r}_1(e) = h_e^{1/2}\|\lambda_h - \partial_{\nu}u_h\|_{0,e} = h_e^{1/2}\|\gamma h_e^{-1}(g - u_h)\|_{0,e} := \gamma\mathbf{r}_3(e),$$

with

$$\mathbf{r}_3(e) = h_e^{-1/2}\|u_h - g\|_{0,e},$$

which, combining with (2.28) and (3.7), yields

$$(3.11) \quad \sum_{e \in \mathcal{E}_h^b} \int_e (\lambda_h - \partial_{\nu}u_h)(z - \hat{\Pi}_h z) \mp \gamma^{-1} \sum_{e \in \mathcal{E}_h^i} h_e \int_e (\nabla u_h \cdot \nu - \lambda_h)(\nabla(\hat{\Pi}_h z) \cdot \nu) \lesssim \sqrt{\sum_{e \in \mathcal{E}_h^b} (1 + \gamma^2)|\mathbf{r}_3(e)|^2}.$$

Collecting all, we obtain the following a posteriori error bound for the normal flux computed using Nitsche's method.

$$(3.12) \quad \|\partial_{\nu}u - \lambda_h\|_{-1/2,\Gamma} \lesssim \sqrt{\zeta_T^2 \sum_{T \in \mathcal{T}_h} |\mathbf{r}(T)|^2 + \sum_{e \in \mathcal{E}_h^i} \zeta_e^2 |\mathbf{r}_0(e)|^2 + \sum_{e \in \mathcal{E}_h^b} (1 + \gamma^2)|\mathbf{r}_3(e)|^2 + \sum_{P \in \mathcal{N}_h^b} \sum_{e \subseteq \Delta_P} |\mathbf{r}(e, P)|^2},$$

where  $\lambda_h$  is given in (3.10).

**4. Numerical experiments.** In the computation, we approximate  $\rho_K$  by the following:

$$\rho_K \approx \min_{x \in \mathcal{N}_{\Delta_K}} d_{\Gamma}(x)$$

where  $\mathcal{N}_{\Delta_K}$  is the set of all vertices on  $\Delta_K$ . For simplicity, we fix  $C_1 = 1$ .

Firstly we demonstrate the action of the weight  $\zeta_T$  defined in (2.22) by showing its effect on the adaptive mesh based solely on such a quantity, independently of any particular problem. We start with a 4 by 4 initial triangular mesh on a unit square domain, see Figure 1(a). A total number of 7 refinement steps are performed, with the refinement strategy set such that an element  $K$  is refined if

$$\zeta_T > 0.5\zeta_{T,max}, \quad \zeta_{T,max} = \max_{T \in \mathcal{T}_h} \zeta_T.$$

Figure 1 shows the meshes at various steps. We observe that as mesh gets finer, more refinements are located near the boundary. Further experiments also show that the smaller the  $C_2$  and the higher the order  $k$ , the refinements on the boundary will become more dominant.

**4.1. Computation of the true error.** To verify the performance of our algorithm, we need to compute the true error, that is  $\|\lambda - \lambda_h\|_{-1/2,\Gamma}$ . By definition,

$$\|\lambda - \lambda_h\|_{-1/2,\Gamma}^2 = |\nabla w|_{\Omega}^2 = \langle \lambda - \lambda_h, w \rangle_{\Gamma}$$

where  $w \in H^1(\Omega)$  satisfies the following variational problem:

$$(4.1) \quad \int_{\Omega} \nabla w \cdot \nabla v = \int_{\Gamma} (\lambda - \lambda_h)v, \quad \text{and} \quad \int_{\Omega} w \, dx = 0.$$

Note that ((4.1)) is a pure Riemann problem. The compatibility of the solution is guaranteed since  $\int_{\Gamma} (\lambda - \lambda_h) \, ds = 0$  for all numerical methods. We approximate the true error in each refinement step

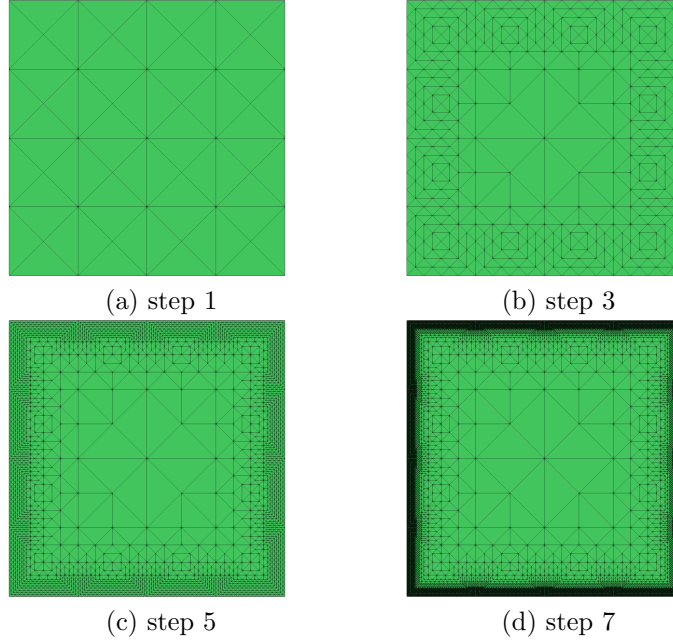


Fig. 1: Adaptive meshes based on  $\varsigma_T$  with  $k = 2$  and  $C_2 = 0.01$

using a two order higher finite element method on a finer mesh (as compared to the mesh size). We let  $w_h \in V_h^{k+2}$  denote the Galerkin projection of  $w$  on  $V_h^{k+2} = \{v \in H^1(\Omega) : v|_K \in P^{k+2}(K) \quad \forall K \in \tilde{\mathcal{T}}_h\}$ . Here  $\tilde{\mathcal{T}}_h$  is the finer mesh. We then approximate the error by

$$(4.2) \quad \|\lambda - \lambda_h\|_{-1/2, \Gamma}^2 \approx |\nabla w_h|_{\Omega}^2 \quad (\text{or } \int_{\Gamma} (\lambda - \lambda_h) w_h).$$

When  $\lambda$  does not have enough regularity, using ((4.2)) to accurately compute the true error becomes infeasible as a very fine mesh is required to guarantee the accuracy. We therefore introduce another method to compute the true error by exploiting the properties of the wavelet decomposition. Indeed, it is known that, by expanding a function in  $H^{-1/2}(\Gamma)$  based on a suitable wavelet basis, an equivalent  $H^{-1/2}(\Gamma)$  norm can be computed by taking a weighted  $\ell^2$  norm of the coefficient vector. The latter can be efficiently computed by applying a wavelet transform [13]. This only requires computations on  $\partial\Omega$ , therefore we are able to compute the true error to a satisfactory accuracy even for low regularity  $\lambda$ .

More precisely, given  $v \in H^{-1/2}(\Gamma)$ , we aim at computing  $\|v\|_{-1/2, \Gamma}$ . In order to do so, we consider the sequence of spaces  $\{V_j\}_{j=0}^{\infty}$  such that  $V_j \subset L^2(\Gamma)$  is the space of piecewise constant functions on the embedded uniform grid on  $\Gamma$  with mesh size  $|\Gamma|2^{-j}$ . We denote by  $\{x_k^j\}_{k=0}^{2^j-1}$ , the nodes of the corresponding mesh, which we assume to be ordered counter-clock wise. For  $v \in V_j$ , we can compute the vector  $\mathbf{v}_j$  of length  $2^j$

$$\mathbf{v}_j := \{v_{jk}\}_{k=0}^{2^j-1} \quad \text{and} \quad v_{jk} = \frac{2^{j/2}}{|\Gamma|} \int_{x_k^j}^{x_{k+1}^j} v.$$

$\{v_{jk}\}_{k=0}^{2^j-1}$  is regarded as the coefficients of the  $L^2(\Gamma)$  orthonormal bases consisting of the normalized characteristic functions on the elements of the grid. As  $V_j \subset V_{j+1}$ , for all level  $j$  we can decompose  $v_{j+1} \in V_{j+1}$  as  $v_{j+1} = v_j + d_j$ , with  $v_j \in V_j$  obtained by applying a suitable oblique projector  $P_j$  to  $v_{j+1}$ . This gives us a telescopic expansion of all function in  $V_M$  as  $v_M = v_0 + \sum_{j=0}^{M-1} d_j$ , and, passing to the limit as  $M$  goes to infinity, of all functions in  $L^2(\Gamma)$  as  $v = v_0 + \sum_{j=0}^{\infty} d_j$ . Given  $\mathbf{v}_{j+1}$ , we can compute  $\mathbf{v}_j := \{v_{jk}\}_{k=0}^{2^j-1}$  and  $\mathbf{d}_j := \{d_{jk}\}_{k=0}^{2^j-1}$  (this last one being the vector of coefficients of  $d_j$  with respect to a suitable basis for the space  $W_j = (1 - P_j)V_{j+1}$ ), by applying a *low-pass filter*  $h$  (strictly related with the projector  $P_j$ ), and the *band-pass filter*  $g = [1, -1]$ :

$$v_{jk} = \sum_{l=0}^L \frac{\sqrt{2}}{2} h(l) v_{j+1,2k+l} \quad \text{and} \quad d_{jk} = \sum_{l=0}^1 \frac{\sqrt{2}}{2} g(l) v_{j+1,2k+l} = \frac{\sqrt{2}}{2} (v_{j+1,2k} - v_{j+1,2k+1}),$$

where  $L + 1$  is the length of the low-pass filter  $h$ . In the above computation the function  $v$  is considered as periodic, so that, when the index  $2k + l > 2^{j+1} - 1$ , we extend the vector  $\mathbf{v}_{j+1}$  as  $v_{j+1,2^{j+1}+k} = v_{j+1,k}$ ,  $k \geq 0$ . For suitable choices of the low pass filter  $h$ , the following norm equivalence holds for all  $v \in H^{-1/2}(\Omega)$  ([14])

$$\|v\|_{-1/2,\partial\Omega}^2 \simeq \|\mathbf{v}_0\|_2^2 + \sum_{j=0}^{\infty} 2^{-j} \|\mathbf{d}_j\|_2^2,$$

where  $\|\cdot\|_2$  denotes the Euclidean norm on  $\mathbb{R}^{2^j}$ . In our experiments we choose the so called *(2,2)-biorthogonal wavelet* (see [13]), for which the low pass filter  $h$  is

$$h = \frac{\sqrt{2}}{2} [3/128, -3/128, -11/64, 11/64, 1, 1, 11/64, -11/64, -3/128, 3/128].$$

By choosing  $M$  big enough and projecting  $v$  onto  $V_M$  (in our tests we use the  $L^2$  orthogonal projection), we approximate the norm by

$$(4.3) \quad \|v\|_{-1/2,\partial\Omega}^2 \approx \|v_0\|_2^2 + \sum_{j=0}^{M-1} 2^{-j} \|d_j\|_2^2.$$

## 4.2. Test results.

*Example 4.1.* In this example, we test the algorithm with the Franke function [18] on the unit square domain,

$$\begin{aligned} u(x, y) = & 0.75 \exp(-(9x-2)^2/4 - (9y-2)^2/4) + 0.75 \exp(-(9x+1)^2/49 - (9y+1)/10) \\ & + 0.5 \exp(-(9x-7)^2/4 - (9y-3)^2/4) - 0.2 \exp(-(9x-4)^2 - (9y-7)^2). \end{aligned}$$

This function has two peaks at  $(2/9, 2/9)$  and  $(7/9, 1/3)$  and one sink at  $(4/9, 7/9)$ .

We first test the convergence rate of the true error  $\|\lambda - \lambda_h\|_{-1/2,\Gamma}$  on uniform meshes. We compute the true error using the two methods mentioned above and denote by  $E_1$  the error computed by (4.2) and by  $E_2$  the error computed using the wavelet in (4.3) with  $M = 20$ . We solve the problem ((4.2)) on a finer uniform mesh with mesh size  $h = 1/64$ . From Tables Table 1 and Table 2, it can be seen that  $E_2$  can serve as a good alternative for both method and the ratio

Table 1: [Example 4.1](#): Convergence rates for Nitsche's method

h	k = 1				k = 2			
	$E_1$	rate	$E_2$	$E_2/E_1$	$E_1$	rate	$E_2$	$E_2/E_1$
1/8	3.35E-1	0.40	8.53E-2	0.25	2.86E-1	3.31	5.17E-2	0.18
1/16	1.73E-1	0.95	4.51E-2	0.26	3.19E-2	3.16	7.50E-3	0.23
1/32	8.66E-2	1.00	2.26E-2	0.25	4.69E-3	2.77	1.44E-3	0.30
1/64	4.33E-2	1.00	1.13E-2	0.26	2.51E-4	2.10	8.15E-5	0.32

Table 2: [Example 4.1](#): Convergence rates for Lagrangian Multiplier method

h	k = 2, k' = 0			
	$E_1$	rate	$E_2$	$E_2/E_1$
1/8	4.58E-2	1.88	1.14E-2	0.25
1/16	1.43E-2	1.68	3.97E-3	0.28
1/32	4.80E-3	1.57	1.40E-3	0.29
1/64	5.62E-4	1.54	1.82E-4	0.32

between  $E_2$  and  $E_1$  is relatively stable around 0.25 (the fluctuation of the ratio is probably caused by the inaccurate computation of  $E_1$ ).

We now test the adaptive mesh refinement procedure for Lagrangian method. In the adaptive procedure, we set the stopping criteria such that the total number of DOFs less than 20,000. The marking strategy is set such that an element  $K$  is refined if  $\eta_K \geq 0.5\eta_{K,max}$ . In this example, we also set  $C_2 = 0.01$ . The initial mesh is set to be the  $4 \times 4$  mesh in [Figure 1\(a\)](#). We compare our error estimator with the classical residual based error estimator without the extra weight  $\zeta_T$ . For the Lagrangian method it is defined as

$$\eta_{classical} = \left( \sum_K h_K^2 \|f + \Delta u\|_K^2 + \sum_{F \in \mathcal{E}_h^i} h_F \|\partial_\nu u_h\|_F^2 + \sum_{F \in \mathcal{E}_h^b} (h_F^{-1} \|g - u_h\|_F^2 + h_F \|\partial_\nu u_h - \lambda_h\|_F^2) \right)^{1/2}.$$

and for Nitsche's method as

$$\eta_{classical} = \left( \sum_K h_K^2 \|f + \Delta u\|_K^2 + \sum_{F \in \mathcal{E}_h^i} h_F \|\partial_\nu u_h\|_F^2 + \sum_{F \in \mathcal{E}_h^b} \gamma^2 h_F^{-1} \|g - u_h\|_F^2 \right)^{1/2}.$$

It is well known that  $\eta_{classical}$  is optimal in minimizing the energy norm of the error, i.e.,  $\|\nabla(u - u_h)\|$ .

[Figure 2](#) shows the final meshes for the AMR procedure using respective  $\eta_{classical}$  (left) and  $\eta$  (right). It can be seen that [Figure 2\(left\)](#) has dense refinements around the peaks and sinks while [Figure 2\(right\)](#) has dense refinements near the boundary and ignores the peaks and sinks in the interior domain.

In [Figure 3a–Figure 3c](#), we compare the convergence of the error and estimators. In terms of total degree of freedoms (DOFs). From [Figure 3a](#) we see that the error driving by  $\eta$  converges faster than that by  $\eta_{classical}$  which is about the order  $N^{-1}$  with N being the total number of DOFs.



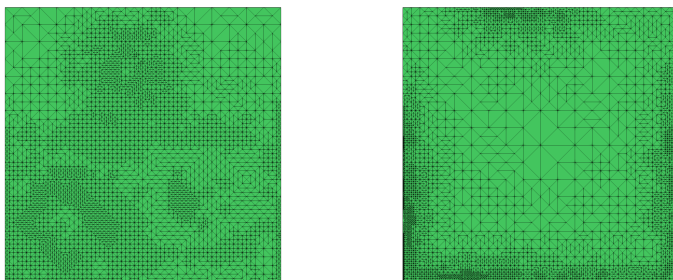


Fig. 2: Example 4.1. The final meshes for Lagrangian method ( $k = 2, k' = 0$ )

Figure 3b shows that both errors converge optimally with respect to the number of boundary DOFs. However, much more DOFs are located on the boundary by  $\eta$  providing total number of DOFs are similar. Figure 3c shows that the ratio between the local DOFs and the total DOFs gradually gets higher for the meshes generated by  $\eta$  in the AMR procedure.

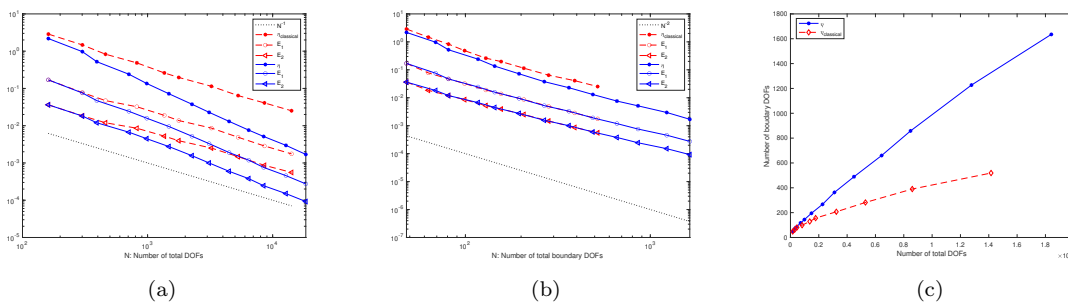


Fig. 3: Example 4.1. Convergence of estimators and true error for Lagrangian method ( $k = 2, k' = 0$ )

We now move to test the Nitsche's method with  $k = 1$  and  $k = 2$ . For the parameters, we set  $\gamma = 10$ . Figure 4 compares the final meshes generated using Nitsche's method using  $\eta$  and  $\eta_{classical}$ . We observe similar phenomena as using Lagrangian method, i.e., the mesh generated by  $\eta_{classical}$  has dense refinement near the peaks and sinks while the mesh generated by  $\eta$  has dense refinements all near the boundary. The convergence of the true error and error estimators are plotted in Figure 5.

Both Figure 3a and Figure 5 indicate that  $E_2$  can serve as a good alternative to  $E_1$  in the adaptive procedure. The ratio  $E_2/E_1$  is all around 0.25. In the remaining examples, we will use  $4 * E_2$  as the true error.

In Figure 6, we compare the convergence of energy error using  $\eta_{classical}$  and  $\eta$ . It can be seen that  $\eta_{classical}$  serves as a good error indicator for the energy error while  $\eta$  does not yield optimal convergence for the energy error.

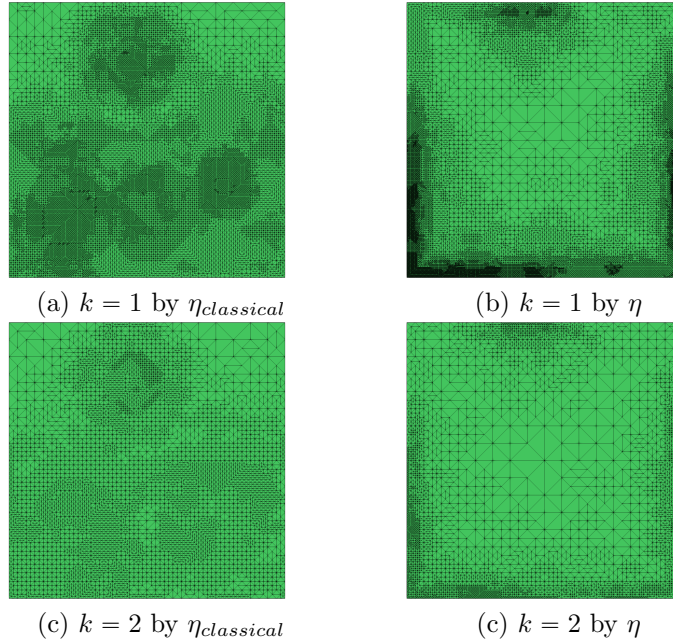


Fig. 4: [Example 4.1](#). Final meshes using Nitsche's method.

*Example 4.2.* In this example, we test a problem with a strong interior peak. The true solution has the following representation:

$$u(x, y) = \exp(-\alpha_p * ((x - x_p)^2 + (y - y_p)^2))$$

where  $\alpha_p = 200$ ,  $x_p = 0.2$  and  $y_p = 0.2$ . This function has a peak at the point  $(x_p, y_p)$

In the AMR procedure, the stopping criteria is set such that the total number of DOFs less than 20,000. We firstly test the Lagrangian method and set  $C_2 = 0.1$ . Then we test the Nitsche's method for the first and second orders. To test the robustness of the algorithm with respect to  $C_2$ , we set  $C_2 = 0.01$  and 0.5 for the first and second order, respectively. For [Example 4.2](#), we observe similar numerical results as in [Example 4.1](#), see [Figure 7–Figure 10](#).

*Example 4.3.* In this example, we test the L-shape problem with boundary singularity. The true solution has the following representation in polar coordinates:

$$u(r, \vartheta) = r^\alpha \sin(\alpha\vartheta)$$

where  $\alpha = 2/3$  and the  $\Omega$  being the L-shaped domain, i.e.,  $\Omega = [-1, 1]^2 \setminus (0, 1) \times (-1, 0)$ .

We firstly test the convergence of the error on uniform meshes, see [Table 3](#). The results of the adaptive procedure are presented in [Figure 11–Figure 14](#). In this test, we set  $C_2 = 0.01$ .

**5. Appendix: A high order Clément type projector.** For each triangle  $T$  in the triangulation we consider the canonical basis for the space  $\mathbb{P}_k(T)$ , which we index by the corresponding

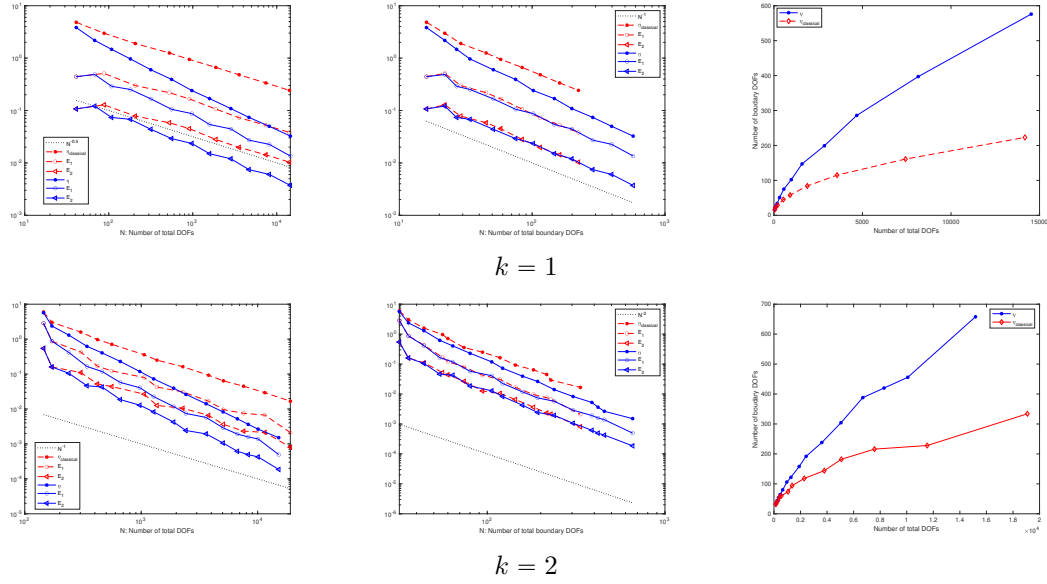
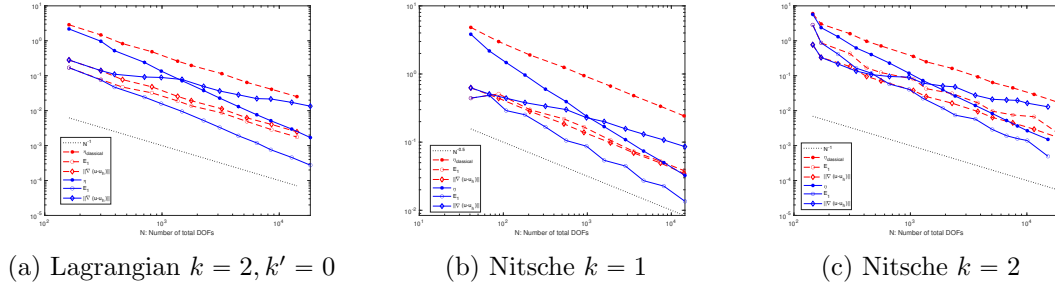


Fig. 5: Example 4.1. Convergence of estimators and true error for Nitsche's method


 Fig. 6: Example 4.1. Comparison of convergence with energy error  $\|\nabla(u - u_h)\|$ 

node,  $\{\mathbf{y}_1^T, \dots, \mathbf{y}_N^T\}$ , with  $N = (k+1)(k+2)/2$  being the dimension of  $\mathbb{P}_k(T)$ . The set  $\{\mathbf{y}_1^T, \dots, \mathbf{y}_N^T\}$  is obtained as the image of a fixed set of unisolvent nodes on a reference triangle  $\hat{T}$ . Denote the basis functions by

$$\mathcal{B}^T = \{\phi_{\mathbf{y}_1}^T, \dots, \phi_{\mathbf{y}_N}^T\}.$$

We also introduce a set of biorthogonal dual bases in the space  $\mathbb{P}_k(T)$  for  $\mathcal{B}^T$

$$\tilde{\mathcal{B}}^T = \{\tilde{\phi}_{\mathbf{y}_1}^T, \dots, \tilde{\phi}_{\mathbf{y}_N}^T\} \text{ such that } \int_T \tilde{\phi}_{\mathbf{y}_i}^T \phi_{\mathbf{y}_j}^T = \delta_{i,j} \quad \forall 1 \leq i, j \leq N.$$

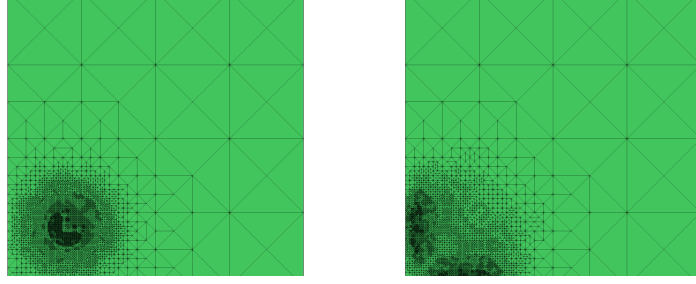


Fig. 7: **Example 4.2.** The final meshes for Lagrangian method ( $k = 2, k' = 0, C_2 = 0.1$ )

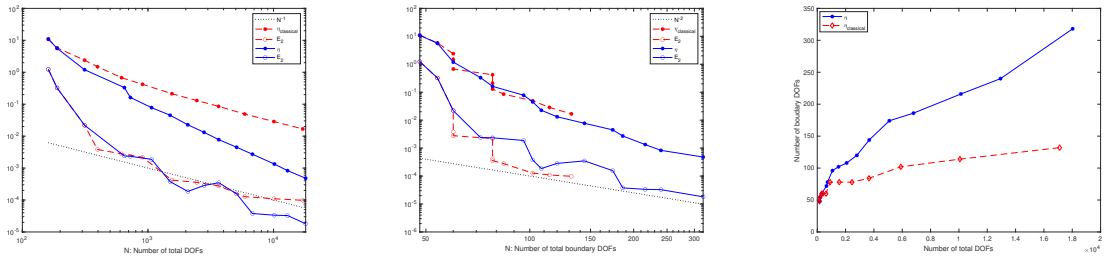


Fig. 8: **Example 4.2.** Convergence of estimators and true error for Lagrangian method ( $k = 2, k' = 0, C_2 = 0.1$ )

Let  $\Pi_k^T : L^2(T) \rightarrow \mathbb{P}_k(T)$  denotes the  $L^2(T)$  projector that takes the form

$$\Pi_k^T(u) = \sum_{i=1}^N \left( \int_T u \tilde{\phi}_{\mathbf{y}_i}^T \right) \phi_{\mathbf{y}_i}^T.$$

Recall that we have the following norm equivalence (which can be proven by a scaling argument, taking advantage of the equivalence of all norms on the finite dimensional space  $\mathbb{P}_k(\hat{T})$ ):

$$(5.1) \quad \left\| \sum_{i=1}^N c_i \phi_{\mathbf{y}_i}^T \right\|_{0,T}^2 \simeq h_T^2 \sum_i |c_i|^2.$$

Moreover, as  $\tilde{\phi}_{\mathbf{y}_i}^T$  is a polynomial in  $\mathbb{P}_k(T)$ , using (5.1), we have

$$\|\tilde{\phi}_{\mathbf{y}_i}^T\|_{0,T} = \sup_{p \in \mathbb{P}_k(T)} \frac{\int_T \tilde{\phi}_{\mathbf{y}_i}^T p}{\|p\|_{0,T}} = \sup_{\mathbf{c} = \{c_j\}_{j=1}^N} \frac{\sum_j c_j \int_T \tilde{\phi}_{\mathbf{y}_i}^T \phi_{\mathbf{y}_j}^T}{\|\sum_j c_j \phi_{\mathbf{y}_j}^T\|_{0,T}} = \sup_{\mathbf{c} = \{c_j\}_{j=1}^N} \frac{c_i}{h_T \|\mathbf{c}\|} \lesssim h_T^{-1}.$$

Let us now consider the global canonical finite element basis

$$\mathcal{B} = \{\phi_{\mathbf{y}} : \mathbf{y} \text{ node of } \mathcal{T}_h\} \quad \text{s.t.,} \quad \phi_{\mathbf{y}}|_T = \begin{cases} \phi_{\mathbf{y}}^T, & \text{when } \mathbf{y} \in \bar{T}, \\ 0, & \text{when } \mathbf{y} \notin \bar{T}. \end{cases}$$

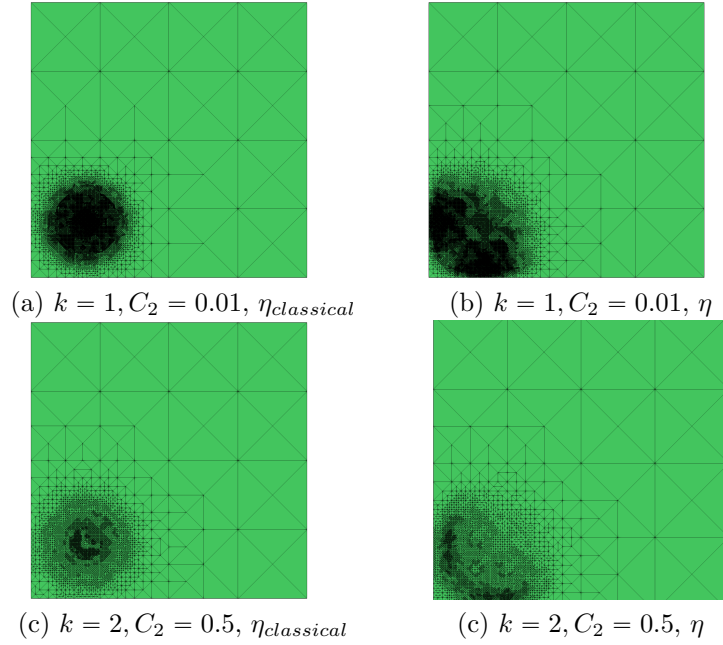


Fig. 9: Example 4.2. Final meshes using Nitsche's method.

Table 3: Example 4.3: Convergence rates on uniform meshes

h	Lagrangian $k = 2$		Nitsche $k = 1$		Nitsche $k = 2$	
	$E_2$	rate	$E_2$	rate	$E_2$	rate
1.76E-1	2.46E-2	1.13	7.66E-2	0.65	1.60E-2	0.34
8.84E-2	1.56E-2	0.65	5.37E-2	0.51	1.10E-2	0.53
4.42E-2	1.00E-2	0.65	3.67E-2	0.54	7.54E-3	0.55
2.21E-2	6.37E-3	0.65	2.48E-2	0.56	5.08E-3	0.57
1.10E-2	4.06E-3	0.65	1.66E-2	0.57	3.39E-3	0.58
5.52E-3	2.59E-3	0.65	1.11E-2	0.58	2.26E-3	0.59

For  $\mathbf{y}$  a node of  $\mathcal{T}_h$ , let  $M_{\mathbf{y}}$  denote the cardinality of the set  $\{T : \mathbf{y} \in \bar{T}\}$ . We define a set of global dual bases as follows.

$$\tilde{\mathcal{B}} = \{\tilde{\phi}_{\mathbf{y}} \in L^2(\Omega), \mathbf{y} \text{ node of } \mathcal{T}_h\} \quad \text{s.t.}, \quad \tilde{\phi}_{\mathbf{y}}|_T = \begin{cases} M_{\mathbf{y}}^{-1} \tilde{\phi}_{\mathbf{y}}^T, & \text{when } \mathbf{y} \in \bar{T}, \\ 0, & \text{when } \mathbf{y} \notin \bar{T}. \end{cases}$$

As our mesh is quasi-uniform we immediately see that for any node  $\mathbf{y} \in \bar{T}$  we have

$$(5.2) \quad \|\phi_{\mathbf{y}}\|_{0, \Delta_T} \lesssim h_T, \quad \|\tilde{\phi}_{\mathbf{y}}\|_{0, \Delta_T} \lesssim h_T^{-1}.$$

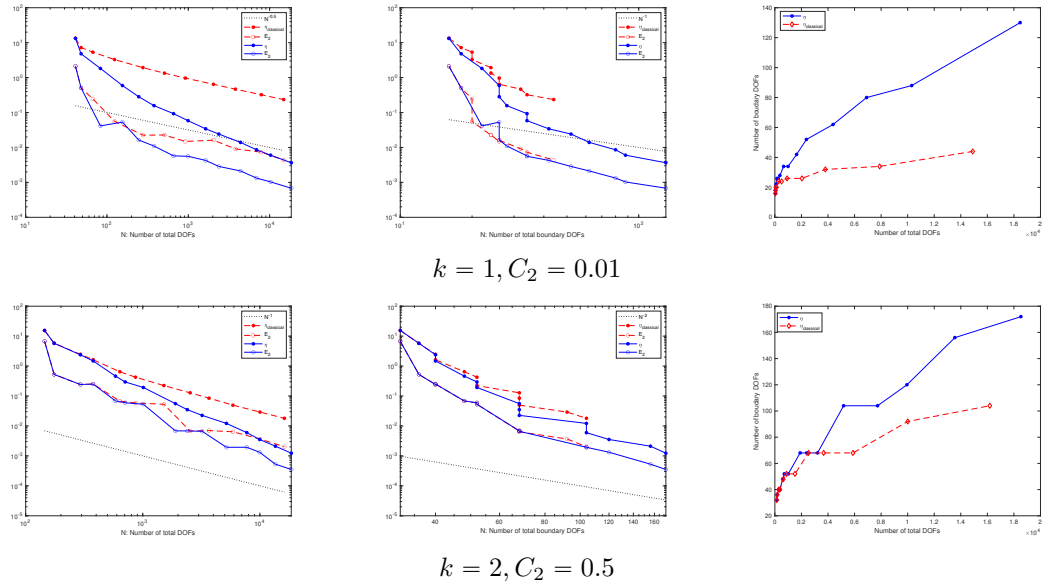


Fig. 10: [Example 4.2](#). Convergence of estimators and true error for Nitsche's method

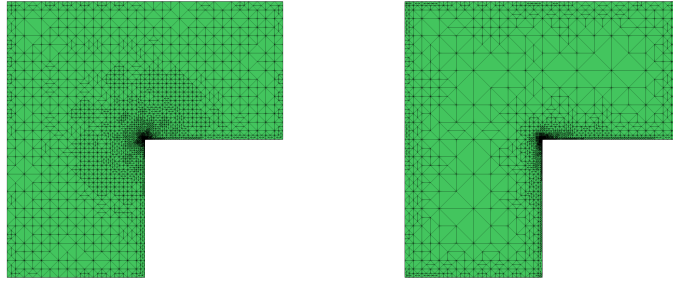


Fig. 11: [Example 4.3](#). The final meshes for Lagrangian method ( $k = 2, k' = 0$ )

It is also easy to check that

$$\int_{\Omega} \tilde{\phi}_{\mathbf{y}} \phi_{\mathbf{y}'} = \sum_{T \in \mathcal{T}_h} \int_T \tilde{\phi}_{\mathbf{y}} \phi_{\mathbf{y}'} = \delta_{\mathbf{y}\mathbf{y}'}$$

The basis  $\tilde{\mathcal{B}}$  is therefore biorthogonal to  $\mathcal{B}$ .

We now define the Clément type projector as  $\hat{\Pi}_h : L^2(\Omega) \rightarrow V_h$  as

$$\hat{\Pi}_h u = \sum_{\mathbf{y}} \left( \int_{\Omega} u \tilde{\phi}_{\mathbf{y}} \right) \phi_{\mathbf{y}}.$$

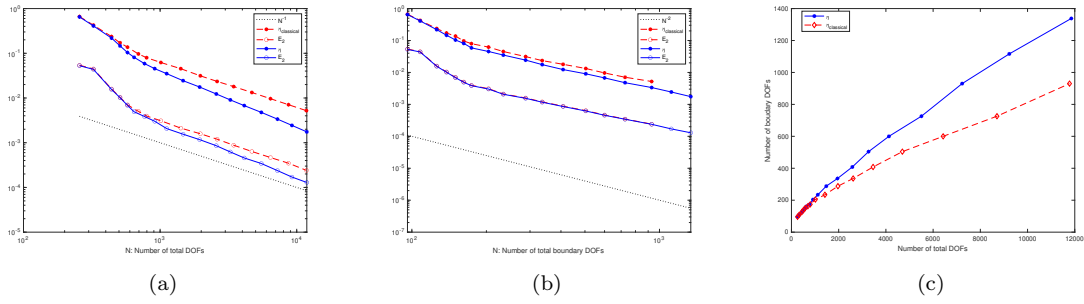


Fig. 12: Example 4.2. Convergence of estimators and true error for Lagrangian method ( $k = 2$ )

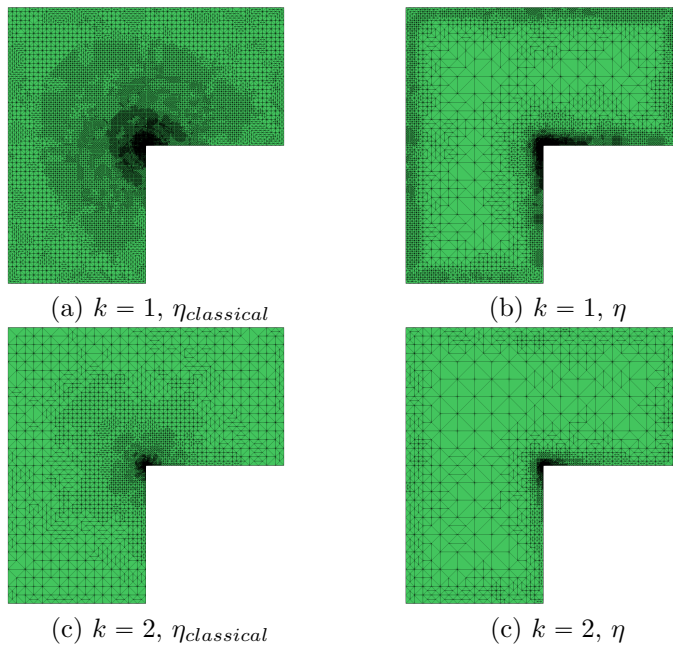


Fig. 13: Example 4.3. Final meshes using Nitsche's method.

The biorthogonality property immediately implies that  $\hat{\Pi}_h$  is a projector, i.e., for all  $v_h \in V_h$

$$\hat{\Pi}_h(v_h) = v_h.$$

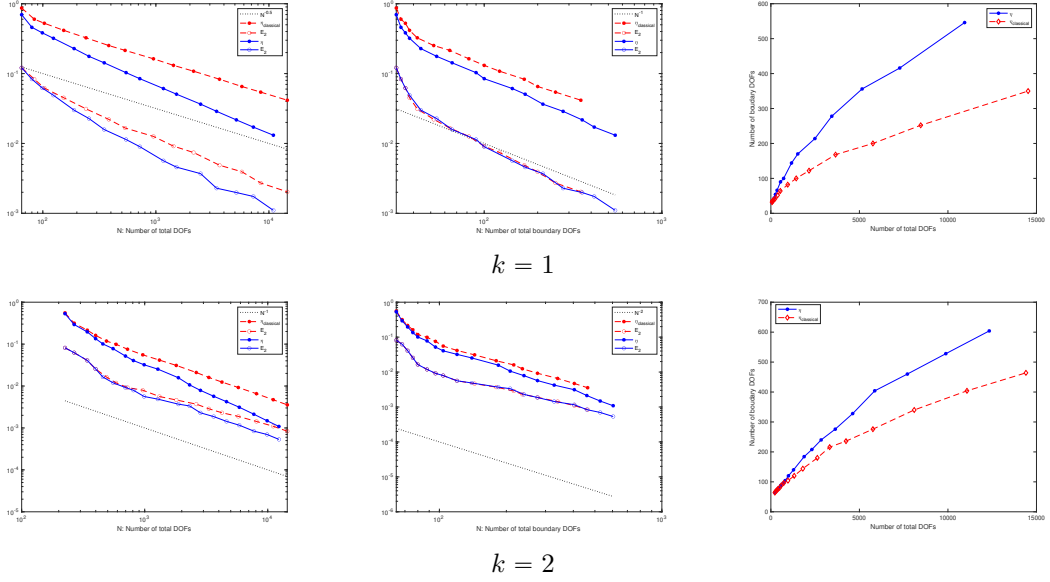


Fig. 14: **Example 4.3.** Convergence of estimators and true error for Nitsche's method

It is also locally stable in  $L^2$  by (5.2), i.e.,

$$\begin{aligned} \|\widehat{\Pi}_h u\|_{L^2(T)}^2 &= \int_T \left| \sum_{\mathbf{y} \in \bar{T}} \left( \int_{\Omega} u \tilde{\phi}_{\mathbf{y}} \right) \phi_{\mathbf{y}} \right|^2 \lesssim \sum_{\mathbf{y} \in \bar{T}} \int_T \left( \int_{\Delta_T} u \tilde{\phi}_{\mathbf{y}} \right)^2 |\phi_{\mathbf{y}}|^2 \\ &\lesssim \|u\|_{0,\Delta_T}^2 \sum_{\mathbf{y} \in \bar{T}} \|\tilde{\phi}_{\mathbf{y}}\|_{0,\Delta_T}^2 \|\phi_{\mathbf{y}}\|_{0,T}^2 \lesssim \|u\|_{0,\Delta_T}^2. \end{aligned}$$

Finally, it locally preserves polynomials: if  $u|_{\Delta_T} = p \in \mathbb{P}_k(\Delta_T)$  then

$$(\widehat{\Pi}_h u)|_T = (\widehat{\Pi}_h p)|_T = p.$$

Thanks to these properties we easily obtain that, for  $0 \leq m \leq k+1$

$$(5.3) \quad \|u - \widehat{\Pi}_h u\|_{0,T} \lesssim h_T^m |u|_{m,\Delta_T}.$$

Moreover, let  $v_h$  denote the  $H^1(T)$  projection of  $u$  over  $\mathbb{P}_k(T)$ . Using a standard argument we can write

$$|\widehat{\Pi}_h u|_{1,T} \leq h_T^{-1} \|\widehat{\Pi}_h u - u\|_{0,T} + h_T^{-1} \|u - v_h\|_{0,T} + |v_h|_{1,T} \lesssim |u|_{1,\Delta_T},$$

which used the fact that the  $H^1$  projector is also locally stable in  $H^1$ . We then easily get

$$|u - \widehat{\Pi}_h u|_{1,T} \leq h_T^{m-1} |u|_{m,\Delta_T},$$

which, combined with (5.3), gives

$$(5.4) \quad \|u - \widehat{\Pi}_h u\|_{0,T} + h_T |u - \widehat{\Pi}_h u|_{1,T} \lesssim h_T^m |u|_{m,\Delta_T} \quad \forall T \in \mathcal{T}_h.$$



## REFERENCES

- [1] M. AKIRA, *A mixed finite element method for boundary flux computation*, Computer methods in applied mechanics and engineering, 57 (1986), pp. 239–243.
- [2] T. APEL, J. PFEFFERER, AND A. RÖSCH, *Finite element error estimates on the boundary with application to optimal control*, Mathematics of Computation, 84 (2015), pp. 33–70.
- [3] T. APEL, J. PFEFFERER, AND M. WINKLER, *Local mesh refinement for the discretization of neumann boundary control problems on polyhedra*, Mathematical Methods in the Applied Sciences, 39 (2016), pp. 1206–1232.
- [4] H. J. C. BARBOSA AND T. J. R. HUGHES, *The finite element method with Lagrange multipliers on the boundary: circumventing the Babuška-Brezzi condition*, Comput. Methods Appl. Mech. Engrg., 85 (1991), pp. 109–128.
- [5] R. BECKER, H. KAPP, AND R. RANNACHER, *Adaptive finite element methods for optimal control of partial differential equations: basic concept*, SIAM J. Control Optim., 39 (2000), pp. 113–132.
- [6] R. BECKER AND R. RANNACHER, *A feed-back approach to error control in finite element methods: basic analysis and examples*, East-West J. Numer. Math., 4 (1996), pp. 237–264.
- [7] R. BECKER AND R. RANNACHER, *Weighted a posteriori error control in FE methods*, IWR, 1996.
- [8] R. BECKER AND R. RANNACHER, *An optimal control approach to a posteriori error estimation in finite element methods*, Acta Numer., 10 (2001), pp. 1–102.
- [9] C. BERNARDI, Y. MADAY, AND A. PATERA, *A new nonconforming approach to domain decomposition: the mortar element method*, in Nonlinear Partial Differential Equations and their Applications, Collège de France Seminar.
- [10] S. BERTOLUZZA, *Local boundary estimates for the Lagrange multiplier discretization of a Dirichlet boundary value problem with application to domain decomposition*, Calcolo, 43 (2006), pp. 121–149.
- [11] S. BERTOLUZZA, *Analysis of a mesh-dependent stabilization for the three fields domain decomposition method*, Numerische Mathematik, 133 (2016), pp. 1–36.
- [12] F. BREZZI, L. P. FRANCA, D. MARINI, AND A. RUSSO, *Stabilization Techniques for Domain Decomposition Methods with Non-matching grids*, Citeseer, 1997.
- [13] A. COHEN, I. DAUBECHIES, AND J.-C. FEAUVEAU, *Biorthogonal bases of compactly supported wavelets*, Communications on Pure and Applied Mathematics, 45 (1992), pp. 485–560.
- [14] W. DAHMEN, *Stability of multiscale transformations*, Journal of Fourier Analysis and Applications, 2 (1996), pp. 341–361.
- [15] B. H. DENNIS AND G. S. DULIKRAVICH, *Simultaneous determination of steady temperatures and heat fluxes on surfaces of three dimensional objects using fem*, ASME-Publications-HTD, 369 (2001), pp. 259–268.
- [16] L. C. EVANS, *Partial Differential Equations*, vol. 19 of Graduate Studies in Mathematics, Providence, 1991.
- [17] B. FAERMANN, *Localization of the aronszajn-slobodeckij norm and application to adaptive boundary elements methods. part i. the two-dimensional case*, IMA journal of numerical analysis, 20 (2000), pp. 203–234.
- [18] R. FRANKE, *A critical comparison of some methods for interpolation of scattered data*, tech. report, Naval Postgraduate School Monterey CA, 1979.
- [19] M. B. GILES, M. G. LARSON, M. LEVENSTAM, AND E. SÜLI, *Adaptive error control for finite element approximations of the lift and drag coefficients in viscous flow*, 1997.
- [20] P. M. GRESHO, R. L. LEE, R. L. SANI, M. K. MASLANIK, AND B. E. EATON, *The consistent galerkin fem for computing derived boundary quantities in thermal and or fluids problems*, International Journal for Numerical Methods in Fluids, 7 (1987), pp. 371–394.
- [21] T. HORGER, J. M. MELENK, AND B. WOHLMUTH, *On optimal  $l_2$ - and surface flux convergence in fem*, Computing and Visualization in Science, 16 (2013), pp. 231–246.
- [22] M. G. LARSON AND A. MASSING,  *$L^2$ -error estimates for finite element approximations of boundary fluxes*, arXiv e-prints, (2014), p. arXiv:1401.6994.
- [23] J. NERG AND J. PARTANEN, *A simplified fem based calculation model for 3-d induction heating problems using surface impedance formulations*, IEEE transactions on magnetics, 37 (2001), pp. 3719–3722.
- [24] J. NITSCHKE, *Über ein variationsprinzip zur lösung von dirichlet-problemen bei verwendung von teilträumen, die keinen randbedingungen unterworfen sind*, Abhandlungen aus dem Mathematischen Seminar der Universität Hamburg, 36 (1971), pp. 9–15.
- [25] J. PFEFFERER AND M. WINKLER, *Finite element error estimates for normal derivatives on boundary concentrated meshes*, SIAM Journal on Numerical Analysis, 57 (2019), pp. 2043–2073.
- [26] T. RICHTER AND T. WICK, *Variational localizations of the dual weighted residual estimator*, Journal of Computational and Applied Mathematics, 279 (2015), pp. 192–208.
- [27] R. STENBERG, *On some techniques for approximating boundary conditions in the finite element method*, J. Comput. Appl. Math., 63 (1995), pp. 139–148.